Hyperfine Interact (2016) 237: 157
DOI 10.1007/s10751-016-1370-x

Development of Mössbauer diffractometer by using nuclear resonant scattering at SPring-8 BL11XU

Shin Nakamura[1] · Takaya Mitsui[2] · Kosuke Fujiwara[3] · Naoshi Ikeda[3] · Yasuhiro Kobayashi[4] · Susumu Shimomura[5]

Abstract A Mössbauer diffractometer has been developed by using ^{57}Fe nuclear resonant scattering apparatus at SPring-8 BL11XU in order to obtain a crystal-site-selective Mössbauer spectrum. A θ-2θ goniometer was newly installed between the nuclear monochromator and a detector. From a single crystal Fe_3O_4 mounted on the goniometer, the 111, 222, and 220 reflected γ-rays were used to collect the diffraction spectra at room temperature. The intensity ratio of the two subspectra, corresponding to A- and B-site Fe ions, changes notably according to the reflection index. The diffraction spectrum is composed of a major absorption spectrum and a minor emission spectrum. The former is given by the γ-ray due to the electron scattering and nuclear absorption, whereas the latter is given by the γ-ray due to the nuclear resonant scattering. Interference effects between these two γ-rays are also seen as line broadenings, asymmetric line shapes, and slope of the base lines. These features can be successfully expressed by a Fano function. We consider that the emission spectrum due to the nuclear resonant scattering represents crystal-site-selective Mössbauer spectrum.

This article is part of the Topical Collection on *Proceedings of the International Conference on Hyperfine Interactions and their Applications (HYPERFINE 2016), Leuven, Belgium, 3–8 July 2016*
Edited by Kristiaan Temst, Stefaan Cottenier, Lino M. C. Pereira and André Vantomme

✉ Shin Nakamura
shin@koala.mse.teikyo-u.ac.jp

[1] Department of Science and Engineering, Teikyo University, Utsunomiya 320-8551, Japan

[2] National Institutes for Quantum and Radiological Science and Technology, 1-1-1 Kouto, Sayo-cho, Sayo-gun, Hyogo 679-5148, Japan

[3] Okayama University, 1-1-1, Tsushima-Naka, Kita-ku, Okayama 700-8530, Japan

[4] Research Reactor Institute, Kyoto University, 2-1010 Asashironishi, Kumatori-cho, Sennan-gun, Osaka 590-0494, Japan

[5] Kyoto Sangyo University, Motoyama, Kamigamo, Kita-ku, Kyoto, 603-8555, Japan

Keywords Mössbauer diffractometer · ^{57}Fe nuclear resonant scattering · Crystal-site-selective spectrum · θ-2θgoniometer · Fe_3O_4 · Fano function

1 Introduction

^{57}Fe Mössbauer spectroscopy is a local and dynamic probe having observation time of 10^{-8} s and energy resolution of 10^{-9} eV, which provides not only the electronic state of Fe, but also the magnetic structure and local crystallographic structure around Fe. In many materials containing multi-Fe-sites, their Mössbauer spectra are composed of superposition of the corresponding subspectra. This often makes it difficult to analyze precisely the spectrum and to obtain precise Mössbauer parameters. On the other hand, diffraction measurements, such as X-ray and neutron diffraction, provide information on each crystallographic site, because their intensities are given by the structure factor of constituent atoms. The combination of both techniques, i.e., Mössbauer diffraction, enables us to deduce a specific spectrum only corresponding to the crystallographic site of interest. There have been reported several Mössbauer diffraction studies conducted by using a radioactive source [1–5], but the incident γ-ray seems not to have enough parallelity and intensity in order to obtain a site-selective spectrum in a practical collecting time. At SPring-8 BL11XU, ^{57}Fe nuclear resonant scattering apparatus is in operation. The γ-ray emitted from the $^{57}FeBO_3$ nuclear monochromator has high parallelity (angular divergence within 3”) and high brightness (10^5 times of an usual radioactive source). With Doppler modulation of the nuclear monochromator, we can obtain energy domain Mössbauer spectrum (synchrotron Mössbauer spectroscopy) [6, 7]. This apparatus is very suitable for the Mössbauer diffraction.

In the present research, we have developed the Mössbauer diffractometer by installing a θ-2θ goniometer between the nuclear monochromator and a detector. Specific spectra by using selected γ-ray reflections were measured for a typical multi-Fe-sites compound, magnetite (Fe_3O_4). Magnetite has a cubic inverse-spinel structure (space group $Fd\bar{3}m$, lattice constant $a = 8.396$ Å at room temperature) with Fe^{3+} ions on the A-site (8a) and equal number of $Fe^{2+}$and Fe^{3+} ions on the B-site (16d). We have obtained an evidence for the crystal-site-selective Mössbauer spectrum.

2 Experiments

The ^{57}Fe nuclear resonant scattering apparatus at SPring-8 BL11XU was used to develop the Mössbauer diffractometer. The schematic view of the experimental setup is illustrated in Fig. 1. An undulator radiation is first introduced to a liquid-nitrogen-cooled Si(111) double-crystal monochromator followed by a nested high-resolution monochromator (HRM) consisting of asymmetric Si(511) and asymmetric Si(975) channel-cut crystals. The σ-polarized X-ray beam with the energy of 14.4 keV is incident on the (111) plane of a single crystal $^{57}FeBO_3$ (nuclear monochromator). The nuclear monochromator, with an application of a transverse magnetic field of 150 Oe, is kept at 350 K. The π-polarized single line γ-ray (wave length $\lambda = 0.8603$ Å) with line-width of 15.4 neV is emitted from the crystal. The beam size is 1.6 mm (horizontal) x 0.4 mm (vertical) and the angular divergence is 3.0”. Doppler modulation of the nuclear monochromator gives an energy domain Mössbauer spectrum. Usually, the measurements are conducted in transmission geometry [6, 7]. In the present investigation, a θ-2θ goniometer, where a measured specimen is to

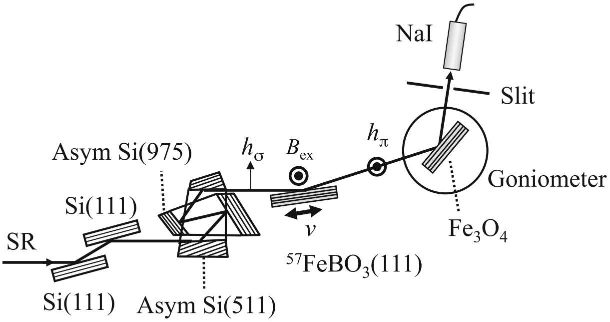

Fig. 1 Schematic view of the experimental setup at Spring-8 BL11XU. $\boldsymbol{h}_\sigma$ and $\boldsymbol{h}_\pi$: unit magnetic field vectors of the incident (σ-polarized) and diffracted (π-polarized) radiations at ^{57}FeBO$_3$ nuclear monochromator, respectively. $\boldsymbol{B}_{ex}$: external field (150 Oe). NaI : scintillation detector

be mounted, is newly installed between the nuclear monochromator and a NaI scintillation detector. Thus a specific spectrum arising only from a selected diffraction point can be measured, which will represent crystal-site-selective Mössbauer spectrum. Details of the experimental setup are presented in ref. [8].

Single crystal specimens of Fe$_3$O$_4$ fabricated by a floating zone melting method (FZ) in a controlled oxygen pressure were used for the measurements. A (111) or (110) plane disc with approximately 5 mm diameter and 1 mm thickness was mounted on the goniometer. Three different reflected γ-rays, 111, 222, and 220 reflections, were used to collect the spectra at room temperature. The collecting time for the measurements using these three reflections were 13, 9.5, and 14 hours, respectively. The Doppler velocity was calibrated in usual transmission geometry (without the goniometer) by using ^{57}Fe metal foil at room temperature.

3 Results and discussions

In Fig. 2a, the rocking curve of the 111 reflection is shown. The Bragg angle is approximately 5.1°and the peak width (FWHM) is approximately 0.11°. The Mössbauer diffraction spectrum collected by using only this reflected γ-ray is shown in Fig. 2b. The spectrum is composed of two subspectra that originate from the A- and B-site Fe ions. Hereafter, we term them the A- and B-site spectra, respectively. Those of the 222 and 220 reflections are shown in Figs. 3a,b and 4a,b, respectively. The Bragg angles of the 222 and 220 reflections are approximately 10.2°and 8.3°, respectively. It is clearly seen that the spectral shape differs each other. Especially, the ratio of the A- and B-site spectra,I_A:I_B, changes notably depending on the reflection index. That is, I_A:I_B for the 111, 222, and 220 reflections are approximately 1:1.5, 1:0.95, and 1:2.5, respectively [see Table 1]. This is an evidence of the crystal-site-selective Mössbauer spectrum. The reflected γ-ray consists of that scattered by the electrons of the atoms at the diffraction point (non-resonant γ-ray) and that scattered by the nuclei after the resonance (resonant γ-ray). The former, combined with nuclear absorption, gives a major absorption spectrum, whereas the latter gives a minor emission spectrum. Hereafter, we call these two γ-rays the electron scattering and the nuclear resonant scattering, respectively, for short. The scattering amplitude of each γ-ray determines the total spectral shape. For example, in an extreme case of a grazing angle incidence where

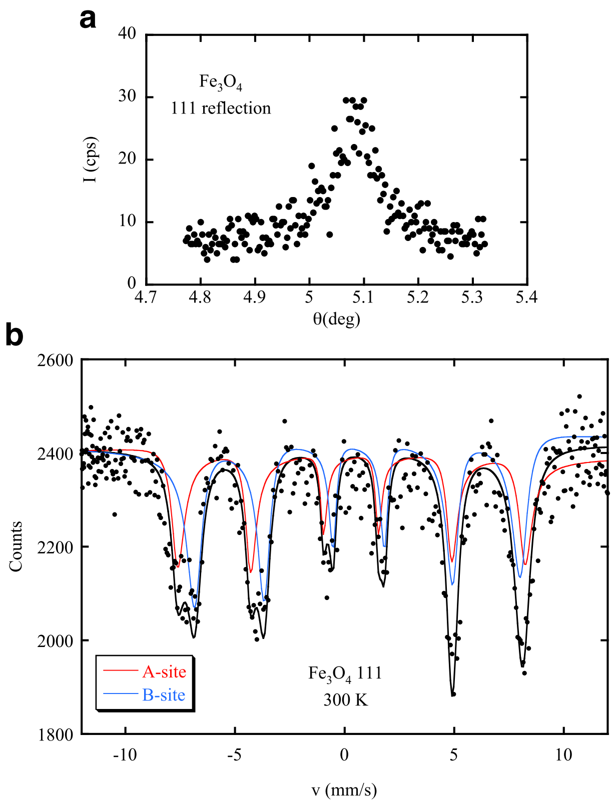

Fig. 2 **a** Rocking curve of the 111 reflection of Fe_3O_4 and (**b**) Mössbauer diffraction spectrum collected by using the 111 reflected γ-ray at room temperature

the nuclear resonant scattering is negligible, purely absorption spectrum is observed [9]. Broadening of the absorption lines, asymmetric line shapes, and slope of the base lines are also recognized. These are results of the interference effect between γ-rays due to the electron scattering and that due to the nuclear resonant scattering. Since the non-resonant and resonant γ-rays coexist on the same reflection path according to the Bragg condition, the interference effect is caused by the quantum effect. The interference effect is especially notable in the 111 reflection spectra, where the first-lines of the A- and B-site spectra overlap remarkably. This may be because both A- and B-site spectra have both scattering components in the case of the 111 reflection [see Table 2] and, in addition, the spectra shapes have opposite asymmetry (constructive and destructive interferences). In such cases, the spectra should be analyzed by using the dynamical theory of diffraction. But in this experiment where the crystallinity of the specimen is not so perfect as seen in rather broad rocking curves of the reflection peaks [see Figs. 2a, 3a, and 4a], a Fano function,

$$I(v) \propto \frac{(\varepsilon + q)^2}{\varepsilon^2 + 1} \tag{1}$$

with

$$\varepsilon = \frac{v - v_0}{W/2},$$

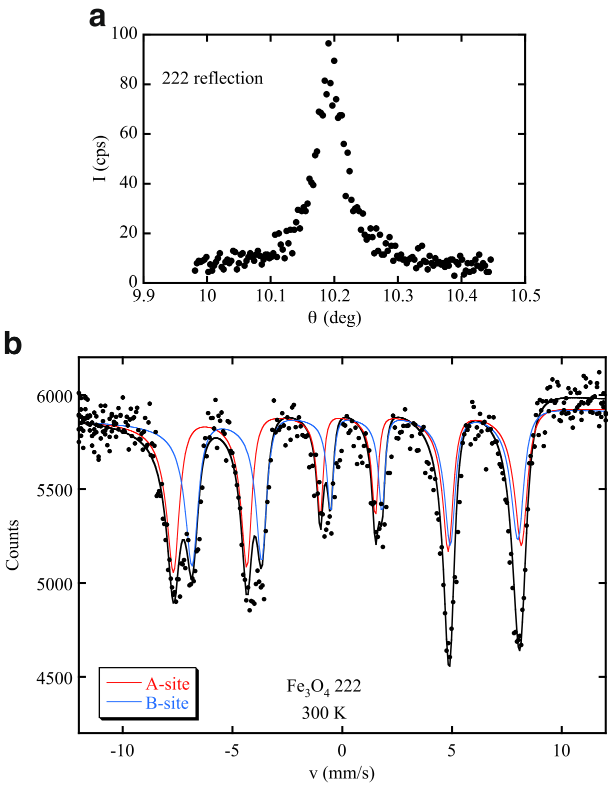

Fig. 3 **a** Rocking curve of the 222 reflection of Fe_3O_4 and (**b**) Mössbauer diffraction spectrum collected by using the 222 reflected γ-ray at room temperature

can be used for the line shapes to analyze the spectra. Here q, v, v_0, and W represent Fano's asymmetric parameter, Doppler velocity, peak position, and line width, respectively. We can successfully analyze the spectra as shown by the smooth curves in Figs. 2b, 3b, and 4b. The absorption line intensity ratios of the sextets are approximately 3:2.5:1:1:2.5:3 for all the three spectra. Although there are four magnetic domains caused by the four [111] magnetic easy axes, slight enhancement of the 2nd-5th line ($\Delta m_{\mathrm{I}} = 0$ transition) intensities is recognized. This indicates that the magnetic moments prefer to lie in the sample plane. The resultant Mössbauer parameters, i.e., isomer shift IS, hyperfine field H_{hf}, quadrupole shift ε_{q}, and outermost line width W, are listed in Table 1. The values are well consistent with those measured in usual transmission geometry by using a radioactive source [10]. Note that the line widths are still rather broad, which may be related to the broad rocking curves of the reflection peaks.

Here we discuss the intensity ratio of the A- and B-site spectra in relation to the reflection index. As we mentioned, the reflection spectra are composed of the major absorption spectra due to the electron scattering combined with nuclear absorption and the minor emission spectra due to the nuclear resonant scattering. We consider that the reflected γ-ray due to the electron scattering does not reveal information of the nuclei at the diffraction point, but just gives usual transmission spectrum during the diffraction path through the specimen. Therefore the intensity ratio of the A- and B-spectra due to the electron scattering, $I_{\mathrm{eA}}:I_{\mathrm{eB}}$,

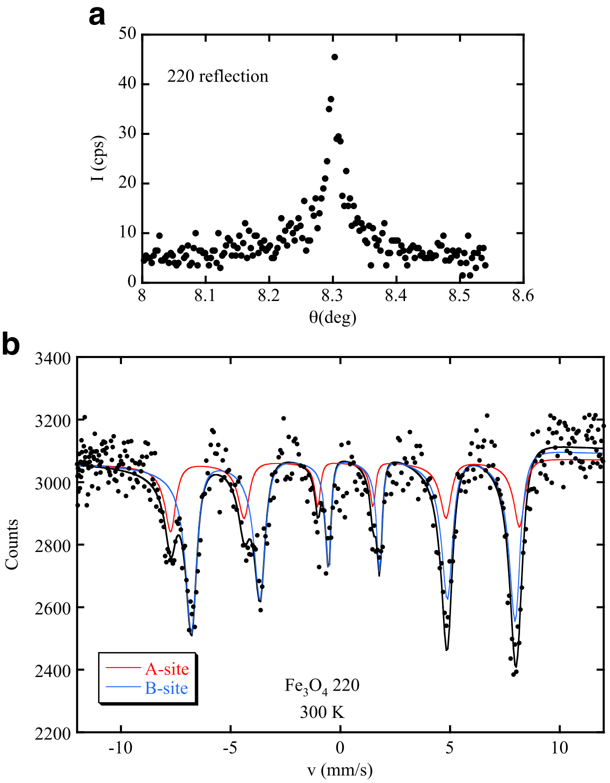

Fig. 4 **a** Rocking curve of the 220 reflection of Fe_3O_4 and (**b**) Mössbauer diffraction spectrum collected by using the 220 reflected γ-ray at room temperature

Table 1 Mössbauer parameters of Fe_3O_4 at room temperature measured in the diffraction geometry: isomer shift *IS*, hyperfine field H_{hf}, quadrupole shift ε_{q}, and outermost line width *W*

Reflection	Site	*IS* (mm/s)	H_{hf} (T)	ε_{q} (mm/s)	*W* (mm/s)	*R* (%)
111	A	0.28(2)	49.2(1)	0	0.70(2)	40(2)
	B	0.65(2)	46.2(1)	−0.02(2)	0.80(2)	60(2)
222	A	0.28(2)	49.2(1)	0	0.70(2)	51(2)
	B	0.64(2)	46.1(2)	−0.02(2)	0.70(2)	49(2)
220	A	0.25(2)	49.4(2)	0	0.60(2)	29(2)
	B	0.64(2)	45.8(2)	−0.01(2)	0.60(2)	71(2)

The quadrupole shift is defined as $\varepsilon_{\mathrm{q}} = (\Delta_{56}\text{-}\Delta_{12})/4$, where Δ_{ij} represents splitting between i-th and j-th absorption lines

should be equal to the crystallographic occupancy of Fe ions, ideally 1:2 in a thin absorber case, regardless of the reflection index. In this experiment, since the penetration depth of the γ-ray is about 10 μm, the transmission path in the specimen is ranging from 100 to

Table 2 The phase factor in the structure factor of the nuclear resonant scattering, $\sum_\rho \exp[i(\mathbf{k}_1 - \mathbf{k}_0) \cdot \mathbf{r}_\rho]$, of A- and B-sites for the 111, 222, and 220 reflections of Fe_3O_4

Reflection	Phase factor of the A-site	Phase factor of the B-site	$\lvert F_{\mathrm{nA}}\rvert^2 : \lvert F_{\mathrm{nB}}\rvert^2$
111	$4(1\text{-}i)$	$4\bar{2}(\text{-}1+i)$	1:2
222	0	$-16i$	0:1
220	8	0	1:0

The ratio of squared value of the structure factor of A- and B-site Fe, $\lvert F_{\mathrm{nA}}\rvert^2 : \lvert F_{\mathrm{nB}}\rvert^2$, is also indicated. Note that the recoilless fractions of the A- and B-site Fe ions are assumed to be the same

200 μm, which causes the saturation effect for the strong absorption lines. We suppose that ratios $I_{\mathrm{eA}}:I_{\mathrm{eB}}$ are approximately 1:1.5 for all the three diffraction spectra (the same ratio obtained for the 111 reflection spectrum). On the other hand, the nuclear resonant scattering can be examined by the structure factor expressed as

$$F_n \propto \sum_\rho \exp[i(\mathbf{k}_1 - \mathbf{k}_0) \cdot \mathbf{r}_\rho] P_{\mathrm{n}}, \tag{2}$$

where $\mathbf{k}_0$, $\mathbf{k}_1$, and $\mathbf{r}_\rho$ represent incident wave vector, reflected wave vector, and position vector of ρ-nucleus, respectively [11]. P_{n} is a polarization factor determined by the unit vectors of the magnetic field of reflected and incident γ-rays, and the unit vector of hyperfine field at the nucleus. The polarization factors of the A- and B-site Fe ions are the same, since Fe_3O_4 has a collinear ferrimagnetic structure. The phase factors of (2), $\sum_\rho \exp[i(\mathbf{k}_1 - \mathbf{k}_0) \cdot \mathbf{r}_\rho]$, for the A- and B-sites are calculated as indicated in Table 2 for the 111, 222, and 220 reflections. The scattered γ-ray intensity is usually proportional to the squared value of the structure factor. Assuming that the recoilless fractions of the A- and B-site Fe ions are the same, the ratios of the squared structure factors of the A- and B-site Fe, $\lvert F_{\mathrm{nA}}\rvert^2 : \lvert F_{\mathrm{nB}}\rvert^2$, are 1:2, 0:1, and 1:0, respectively, for the 111, 222, and 220 reflections. This means that the nuclear resonant scattering spectra for the 222 and 220 reflections consist of only B- and A-site spectrum, respectively. Thus the absorption intensity of the B-site spectrum in the 222 reflection spectrum and that of the A-site spectrum in the 220 reflection spectrum are reduced by the emission spectra due to the nuclear resonant scattering. For the 111 reflection spectrum, the absorption intensity ratio of the A- and B-site spectra is affected little by the nuclear resonant scattering, since $\lvert F_{\mathrm{nA}}\rvert^2 : \lvert F_{\mathrm{nB}}\rvert^2$ is 1:2 (equal to the crystallographic occupancy).

Therefore, in order to obtain the crystal-site-selective Mössbauer spectrum, only the nuclear resonant scattering should be extracted. In other words, the electron scattering should be cut off. The structure factor of the electron scattering is expressed as

$$F_{\mathrm{e}} \propto \sum_\upsilon f_\upsilon \exp\left[i\left(\mathbf{k}_1 - \mathbf{k}_0\right) \cdot \mathbf{r}_\upsilon\right] P_{\mathrm{e}}, \tag{3}$$

with the atomic scattering factor f_υ of υ-element and polarization factor P_{e}. When the incident γ-ray is π-polarized as in the case of this experiment,

$$P_{\mathrm{e}} = \cos 2\theta_{\mathrm{B}}, \tag{4}$$

where θ_B denotes the Bragg angle. Thus selecting the reflection with $\theta_B \approx 45°$, we can suppress the electron scattering, and at the same time we can suppress the interference effect. For this purpose we have two options:

1. Use of the reflection index of the sample having $\theta_B \approx 45°$, e.g., the 888 reflection of Fe_3O_4 ($\theta_B = 45.2°$).
2. Installation of a polarization analyzer between the sample and the counter. As an analyzer crystal, Si(840) plane is suitable ($\theta_B = 45.1°$). The analyzer will cut off the electron scattering regardless of any reflection index of the sample.

We are planning to develop further the Mössbauer diffractometer by using these two options. In any case, the sample should be better prepared by using enriched ^{57}Fe in order to obtain a well-resolved emission spectrum.

4 Summary

We have developed the Mössbauer diffractometer by using ^{57}Fe nuclear resonant scattering apparatus at SPring-8 BL11XU in order to obtain a crystal-site-selective Mössbauer spectrum. The θ-2θ goniometer was newly installed between the nuclear monochromator and the detector. The (111) or (110) plane disc of Fe_3O_4 was mounted on the goniometer and the 111, 222, and 220 reflected γ-rays were used to collect the diffraction spectra at room temperature. The intensity ratio of A- and B-spectra changes notably according to the reflection index. That is, 1:1.5, 1:0.95, and 1:2.5 for the 111, 222, and 220 reflections, respectively. The spectra consist of the contribution from the electron scattering combined with nuclear absorption (gives the major absorption spectrum) and the contribution from the nuclear resonant scattering (gives the minor emission spectrum). Interference effects between the γ-rays due to the electron scattering and that due to the nuclear resonant scattering were also seen as line broadenings, asymmetric line shapes, and slope of the base lines. These features can be successfully expressed by a Fano function. We consider that the emission spectrum due to the nuclear resonant scattering represents a crystal-site-selective Mössbauer spectrum. We are planning to develop further the Mössbauer diffractometer that can cut off the electron scattering.

Acknowledgments This work was supported by the Grants-in-Aid for Scientific Research (C, 26400338) from Japan Society for the Promotion of Science (JSPS). The measurements at SPring-8 BL11XU were performed under the Share Use Program of JAEA Facilities (proposal number 2015A3514) supported by JAEA Advanced Characterization Nanotechnology Platform as a program of ”Nanotechnology Platform” of Ministry of Education, Culture, Sports, Science and Technology (MEXT), Japan.

References

1. Artem'ev, A.N., Perstnev, I.P., Sklyarevskii, V.V., Smirnov, G.V., Stepanov, E.P.: Sov. Phys. JETP **37**, 136 (1973)
2. Artem'ev, A.N., Perstnev, N.P., Sklyarevskii, V.V., Stepanov, E.P.: Sov. Phys. JETP **48**, 587 (1977)
3. Hayashi, N., Sakamoto, I.: Jpn. J. Appl. Phys. **16**, 1713 (1977)
4. von Bürck, U., Smirnov, G.V., Mössbauer, R.L.: J. Phys. C: Solid State Phys. **21**, 5843 (1988)
5. Kovalenko, P.P., Labushkin, V.G., Ovsepyan, A.K., Sarkisov, É..R., Smirnov, E.V., Prokopov, A.R., Seleznev, V.N.: Sov. Phys. Solid State **26**, 1849 (1984)

6. Mitsui, T., Seto, M., Kikuta, S., Hirao, N., Ohishi, Y., Takei, H., Kobayashi, Y., Kitao, S., Higashitaniguchi, S., Masuda, R.: Jpn. J. Appl. Phys. **46**, 821 (2007)
7. Mitsui, T., Hirao, N., Ohishi, Y., Masuda, R., Nakamura, Y., Enoki, H., Seto, M.: J. Synchrotron Rad. **16**, 723 (2009)
8. Mitsui, T., Nakamura, S., Ikeda, N., Fujiwara, K., Masuda, R., Kobayashi, Y., Seto, M.: J. Phys. Soc. Jpn. **85**, 054705 (2016)
9. Mitsui, T., Mibu, K., Seto, M., Kurokuzu, M., Pati, S.P., Nozaki, T., Sahashi, M.: J. Phys. Soc. Jpn. **85**, 063601 (2016)
10. Nakamura, S., Li, L., Tanaka, M., Todo, S., Siratori, K.: J. Phys. Soc. Jpn. **66**, 472 (1997)
11. Smirnov, G.V.: Hyperfine Interact. **125**, 91 (2000)